Vol.41 高等学校化学学报 No.11
2020年11月 CHEMICAL JOURNAL OF CHINESE UNIVERSITIES 2404~2414

[综合评述]

doi: 10.7503/cjcu20200411

长余辉荧光粉在光催化系统中的应用研究进展

苏高鸣, 沈瑞晨, 谈 洁, 袁 荃
(湖南大学化学与化工学院化学生物学与纳米医学研究所,
化学生物传感与计量学国家重点实验室, 长沙 410082)

摘要 长余辉荧光粉是一种新兴的有广泛应用前景的发光材料, 在停止激发后仍可保持发光. 近年来, 具有独特光学性质的长余辉荧光粉得到了发展, 其在光催化领域的应用也得到了广泛的研究. 长余辉材料具有脱离光源的特点, 可以有效地在黑暗环境中推动光催化反应的进行; 同时, 长余辉荧光粉的超长发光寿命使其在长时催化体系中占有重要地位, 使全天候光催化成为可能. 简单来说, 长余辉荧光粉被证明是一种新出现的功能材料, 在光催化方面具有前所未有的优势. 本综述总结了长余辉荧光粉在污染物降解、杀菌消毒和高效制氢领域中应用的最新进展.

关键词 长余辉荧光粉; 光催化; 应用
中图分类号 O643.36; O644.17 **文献标志码** A

Progress on the Application of Long Persistent Phosphors in Photocatalytic System

SU Gaoming, SHEN Ruichen, TAN Jie*, YUAN Quan*
(*Institute of Chemical Biology and Nanomedicine(ICBN), State Key Laboratory of Chemo/Biosensing and Chemometrics, College of Chemistry and Chemical Engineering, Hunan University, Changsha* 410082, *China*)

Abstract Long persistent phosphor is a new and promising luminescent material, which can maintain luminescence after stopping excitation. In the past few years, long persistent phosphors with unique optical properties have been developed and their applications in the field of photocatalysis have been widely studied. Owing to the characteristic of leaving the light source, long persistent luminescence can effectively promote the photocatalytic reaction in the dark environment. Meanwhile, long persistent phosphor has an important position in the long-time catalytic system due to its long luminous life, which makes round-the-clock photocatalysis possible. In brief, long persistent phosphors have been proved to be a new functional material with unprecedented advantages in photocatalysis. In this review, we summarize the latest advances in the application of long persistent phosphors in the degradation of pollutants, sterilization, and efficient hydrogen production.

Keywords Long persistent phosphor; Photocatalysis; Application

收稿日期: 2020-07-01. 网络出版日期: 2020-09-29.
基金项目: 湖南省自然科学基金(批准号: 2020JJ4173, 2020JJ5038)、湖南省科技创新计划项目(批准号: 2018RS3060)和长沙市科技计划项目(批准号: kq1901030)资助.
联系人简介: 袁 荃, 女, 博士, 教授, 主要从事纳米功能材料研究. E-mail: yuanquan@whu.edu.cn
谈 洁, 女, 博士, 副教授, 主要从事纳米功能材料研究. E-mail: tanjie416@hnu.edu.cn

1 Introduction

Long persistent phosphor(LPP) is a class of substances that can absorb solar energy and continue to glow for seconds to days after the excitation stops[1—3]. For nearly a thousand years, human beings have never stopped exploring it. According to ancient Chinese legend, the night pearl formed by natural minerals is regarded as a priceless treasure[3,4]. In the early 17th century, Italian alchemists discovered Bologna stone, which became the first detailed documentation of LPPs. Until 1866, French scientist Sidot first completed the preparation of ZnS:Cu, the LPP gradually faded its mysterious veil and began to attract extensive attention from scientists[5]. In 1996, Matsuzawa *et al.* [2] discovered the famous phosphor $SrAl_2O_4:Eu^{2+},Dy^{3+}$, which can provide bright green light emission within a few hours after the stoppage of excitation, becoming an important milestone in the development of long-persistent materials. $SrAl_2O_4:Eu^{2+},Dy^{3+}$ has a longer afterglow lifetime and higher luminescence intensity than commercial $ZnS:Cu^{2+},Co^{2+}$ materials during the same period. This encouraging finding received a lot of attention, and many researchers began looking for phosphors that emit different colors of light and last longer time. Since then, many LPPs have been developed and widely used in emergency lighting, luminous coatings, instrument display and other fields[6—10].

With the in-depth study of the long afterglow phenomenon and the rapid development of long persistent phosphor, its application areas have also been expanded[11—16]. In recent years, LPPs have shown unprecedented advantages in the field of photocatalysis due to their long luminous life and luminescence without light sources. The basic process of photocatalysis, simply put, is that under the irradiation of light, photocatalytic materials produce photo-induced electron-hole pairs, and then these electrons or holes are migrated to the surface of the material for further redox reactions, thus achieving the purpose of purifying pollutants, material synthesis, and solar energy transformation[17,18]. According to this principle, photocatalysts cannot work continuously without the illumination of light source. However, the alternation of day and night due to the rotation of the Earth makes the sunlight cannot meet the requirements of round-the-clock photocatalysis, which becomes one of the main problems that limit the industrial application of photocatalytic technology. Therefore, the combination of long persistent materials and semiconductor catalysts to build a round-the-clock photocatalytic system became an attractive solution[19].

At present, the research on LPP photocatalysis is still in the initial stage. In 2004, Zhang *et al.* [20] first proposed the definition of LPP photocatalysis. They coated $Sr_4Al_{14}O_{25}:Nd,Eu$ phosphors onto TiO_2 catalyst to build a multilayer massive LPP-catalyst composite, which successfully realized the photodegradation of Rhodamine B under dark conditions created by removal of the light source. Since then, although many articles have been continuously reported on the mechanism of photocatalysis[21—25] and the synthesis of long persistent materials[26—36], few have combined long persistent materials with photocatalysis. Therefore, the purpose of this review is to summarize the specific applications of long-persistent materials in the field of photocatalysis, to analyze the important role and unique advantages of long-persistent materials in round-the-clock photocatalysis systems, and to propose possible solutions and prospects based on the existing problems in the current development.

2 Mechanism of Persistent Luminescence and Its Role in Photocatalysis

To better understand the long afterglow phenomenon and its application in photocatalysis, it is necessary to briefly introduce its luminescence mechanism. At present, the mechanism of electron retention in long persistence luminescence is still controversial, which can be found in some previously published works[1,3,37]. This section only introduces the general concept of long persistence luminescence. It is generally believed that

the generation of the long afterglow is related to two types of active centers in LPP: traps and emitters. In LPPs, traps are usually their intrinsic crystal defects or formed by co-doped ions. The material containing traps is also known as the host, and the doped ions are also called activators. The energy of the trap is usually a few electron volts(eV) lower than the conduction band of the host material. The emitters are usually lanthanide or transition metal ions. The formation of persistent luminescence involves four successive steps, which are the generation, capture, release and recombination of carriers, respectively[38]. Qiu *et al.* [39] made a simple description of the above four processes, as shown in Fig. 1. Charge carriers such as electrons and holes are created when effectively excited (electron beams, X-rays, and ultraviolet light). These charge carriers are then captured by traps in the crystal, where they can be stored for a long time. The above process is called optical charging. When stimulated by heat or light, the captured charge carriers escape from the trap and recombine with the emitter to produce what is known as persistent luminescence.

In essence, LPP is not only a luminescent material but also an electron storage material (ESM)[40]. This electron storage material is key to starting a catalytic reaction under dark conditions. Coupling of LPP with photocatalyst provides a storage place for photogenerated charge carriers so that they will not be consumed only by redox reactions that occur on the catalyst surface. In the dark environment, electrons and holes stored in the LPP can directly enter the electrolyte solutions to exert their catalytic activity via an anodic or cathodic reaction[19]. Or excite the emitter ions through recombination, releasing energy in the form of light, acting as a source of light for catalytic reactions[41—45]. For example, Zhou *et al.* [46] proposed the afterglow mechanism in the $Sr_2MgSi_2O_7$:(Eu, Dy)/g-C_3N_4 system. Specifically explaining, when the sunlight illuminated on the phosphor, its charge energy is transferred to the $4f^7$ energy level of Eu^{2+}. Excited by this energy, Eu^{2+} is subsequently migrated from ground state to the $4f^6 5d$ energy level situated in the conduction band, where Eu^{2+} continues to self-ionize and turns into Eu^{3+} accompanied by the separation of free electrons. Dy^{3+} captures the electron and changes into Dy^{2+}, whose ground state is lower than the conduction band. As soon as the irradiation is cut off, the electron would be transferred back to the conduction band from Dy^{2+} and then recombined with Eu^{3+}, causing an emission from $5d$ to $4f$ as a result of thermal activation. Electrons and holes are created soon after the g-C_3N_4 is excited by the fluorescence, and these carriers then migrated to the catalyst surface to form $\cdot OH$ and $\cdot O_2^-$ through reaction with H_2O and O_2. This luminescence assist system can be used for LPP photocatalysis during the day and at night and can be extended to other fields.

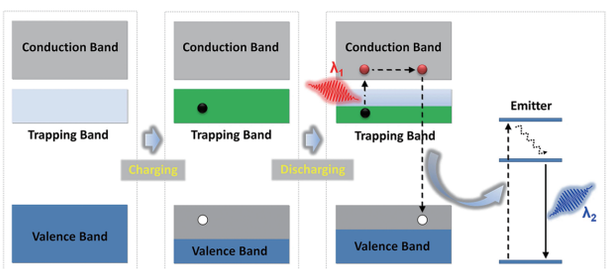

Fig. 1 Brief description of the luminescence mechanism of LPP[39]

Copyright 2014, Springer Nature.

3 Application of LPP Photocatalysis in Degradation of Organic Pollutants

Organic pollutants mainly refer to artificial additives, dyes, pesticides and other substances produced during food processing, textile printing, dyeing and agricultural production. So far, methods including adsorption[47,48], filtration[49], biodegradation[50], chemical catalysis[51] and photocatalysis[52,53] have been successfully developed and applied to organic pollutant treatment. Among these methods, photocatalytic degradation is considered as a new environmental protection technology with good development prospects because of its simple process, easy control of operating conditions, stable and easy obtain of photocatalytic materials, low energy consumption and no secondary pollution. However, three major problems hinder the comprehensive

industrialization of photocatalysis. Firstly, the photocatalytic reaction cannot be carried out in the dark due to the lack of light source which can excite the semiconductor[46,54]. Secondly, due to the light-shielding effect of the solutions[55], particularly in the polluted water body, the light utilization efficiency is low, which means the photocatalyst cannot be fully activated by sunlight. Hence, the formation of photoelectron-hole pair is reduced, which leads to low photodegradation efficiency[56—58]. The last restriction is the unideal performance of photocatalysts. Although extensive studies has been made on TiO_2 due to its cheapness, nontoxicity, and stable optical properties, the practical application is still limited because of its inefficient quantum yield and narrow light response range[59,60].

Recently, some efforts have been made to achieve photocatalytic degradation in wastewater with high catalyst concentration. Zhou *et al.*[61] prepared Zn_2SiO_4: Ga^{3+} single-phase materials with persistent luminescence and catalytic properties by the sol-gel method. With Zn_2SiO_4 as the host, in which only Ga^{3+} ion is doped to replace Zn^{2+} and form an energy trap $GaZn^{+}$ with positive charge to capture photoinduced electrons and slow down the release process of trapped electrons, thus extending the afterglow lifetime to several minutes. The synthesized Zn_2SiO_4: Ga^{3+} has UV afterglow characteristics, emitting a wide fluorescence range from 320 nm to 650 nm under 254 nm excitations, with UV peaks at 362 nm, and the remaining glow signals can remain high intensity for 5 minutes, even can be observed directly with the naked eye in the dark. The total organic carbon (TOC) removal rate of permethrin solution treated with this material was as high as 97% within two hours of UV irradiation, which was significantly superior to 28% of the Zn_2SiO_4 in the blank control group. Considering that Zn_2SiO_4 has been commercialized at low cost, this persistent catalyst will be an ideal material for designing novel photocatalytic reactors at high catalyst concentrations.

Wu *et al.*[62] hybridized silicate-based melilite-type LPP $Sr_2MgSi_2O_7$: Eu^{2+}, Dy^{3+} with a common visible-light-excited photocatalyst, silver orthophosphate (Ag_3PO_4) (Fig. 2). Structural characterization showed that the spherical Ag_3PO_4 nanocrystals in the composites were highly scattered and localized on the tetragonal LPP surface, forming a heterojunction capable of changing the electron transfer behavior (inhibiting carrier recombination), which greatly enhanced the photoactivity of the photocatalyst when externally excited by sunlight and demonstrated long afterglow-driven persistent photocatalysis after shutting down the irradiation. The photodegradation reaction rate constant of $M_{15}A_1$ (the subscript numbers refers to the ratios of phosphors to catalysts) was 0.42 under solar and visible light irradiation, while it was only 0.17 for Ag_3PO_4 itself. After turning off the light source, the photodegradation of methyl orange (MO) by the composite could continue in the dark, driving further decomposition of about 32% of the residual MO in 20 min.

Lu *et al.*[63] added the external rotating disk as the auxiliary to further improve the afterglow lifetime and catalytic activity based on the above two methods. The combination of Cu_2O nanocrystals (NCs) with core-shell structured M-TiO_2 and the incorporation of $SrAl_2O_4$: (Eu, Dy) phosphors enhances the interaction between photons and catalysts by the multiple reflection and scattering of light in M-TiO_2, thus enhancing the 2-Cu_2O NCs/M-TiO_2 light absorption; Meanwhile, the p-n heterojunction between Cu_2O and TiO_2 remarkably inhibits the recombination of electron-hole pairs and is beneficial to capture the photogenerated carriers more effectively. By revolving the catalyst disk, a continuously refreshed slim layer of water film is shaped on the surface of the reactor. The propagation distance of photons in the film is notably shortened, which makes it less easy for the light to be absorbed by the solution, thus improving the light utilization efficiency of the photocatalytic system. LPPs can store excess light energy and produce persistent fluorescence. The composite is excited in the dark so that it remains catalytic for 3 h after removing the light source. The Cu_2O NCs/M-TiO_2 rotating disk reactor incorporating LPPs can achieve round-the-clock photocatalytic degradation of Bisphenol-A and Rhodamine B.

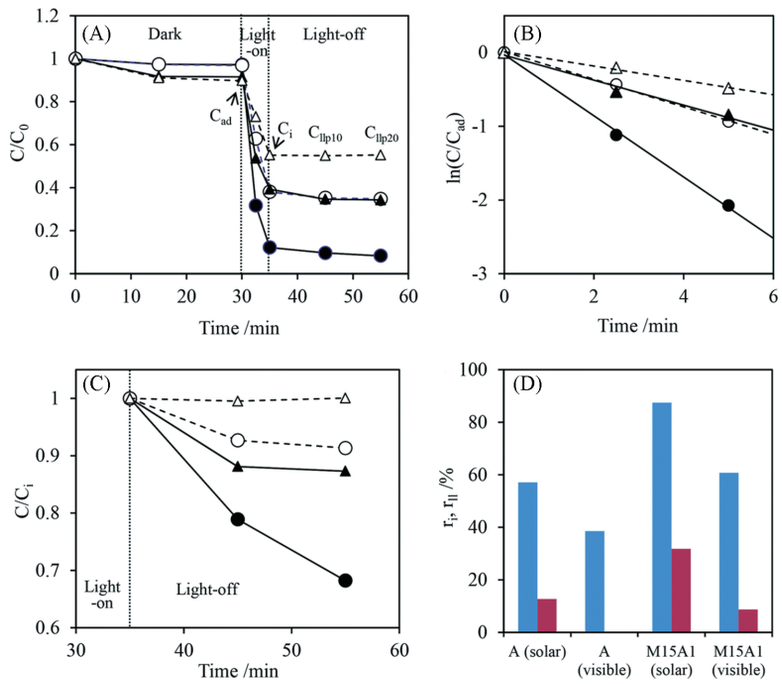

Fig. 2 Degradation of methyl orange using $Sr_2MgSi_2O_7$: Eu^{2+}, Dy^{3+} LLP - Ag_3PO_4 composites during the photocatalytic time process, in which the simulated sunlight(●, ▲) and visible light(○, △) were firstly used for illumination, followed by the removal of light source(A), the MO concentration-time curves of A(▲, △) and M15A1(●, ○) in illumination stage(B) and long afterglow stage(C), where M15A1 refers to a mass ratio of LPP/Ag_3PO_4=15, bar graph of the degradation efficiency during the whole photocatalytic process, where the blue bar and red bar represent the illumination and long persistent stage, respectively(D)[62]

Copyright 2017, Royal Society of Chemistry.

4 Application of LPP Photocatalysis in Disinfection and Sterilization

In the process of seawater desalination, the accumulation of bacteria and microorganisms on the surface of the filter membrane is often the main cause of energy consumption and biological pollution[64,65]. Pre-sterilized treatment can effectively decrease energy consumption and control biological pollution. However, conventional chemical disinfectants such as hypochlorite may destroy the filter membrane, reduce its life, thus increase the desalination cost[66]. By contrast, the use of pure physical ultraviolet light to kill bacteria and microorganisms has obvious advantages[67]. There are three bands of ultraviolet light, in which the UV-C band with a wavelength between 200—275 nm, also called short-wave sterilized UV light, can destroy the molecular structure of microorganisms deoxyribonucleic acid (DNA) or ribonucleic acid (RNA) so that bacteria will die or cannot reproduce, thus achieving the purpose of sterilization. Along with the invention of semiconductor light-emitting diode, UVC LED gradually replaced the mercury lamp and became the representative of modern new disinfection technology, among which phosphors also played an important role[68]. Phosphors in the UVC LED are usually based on the principle of upconversion, which adjusts the visible light to the UVC band, thus making its effort in disinfection and sterilization. However, most of the long persistent phosphors found so far are only in the visible and near-infrared regions[69—71], while there are only less than 20 long afterglow materials with ultraviolet luminescence[72—76]. In recent years, scientists are constantly looking for UVC LPPs and developing their applications in disinfection and sterilization.

Yang *et al.* [77] chose the CS_2NaYF_6 as host (Fig. 3). The wide bandgap characteristics of this material

make it easy to form defects and capture electrons. Pr^{3+} ion is a suitable choice of emitter for the reason that Pr^{3+} ions can release UVC light when a transition occurs between $4f5d$ and $4f^2$. By combining the above two materials, they synthesize micron-sized LPPs with a nominal composition of $Cs_2NaY_{(1-x)}F_6:xPr^{3+}$ using the solid-phase method. The phosphor exhibits a strong, persistent UVC emission peak near 250 nm after X-ray irradiation, and its signal intensity can be maintained within 2 h and still significantly stand above the background interference. Their study on the LPP structure shows that this UVC LPP has a variety of traps, which can not only release shallow electrons at room temperature but also release a great number of electrons confined to deep traps by laser irradiation with different energies. The different defect levels may originate from the introduction of oxygen in the Cs_2NaYF_6 lattice, thus creating a variety of oxygen, fluorine anion vacancies that enable them to catch and store massive amounts of electrons under X-ray irradiation and improve catalytic activity. Three defect models are envisaged as theoretical explanations. To demonstrate this concept, they tested the inactivation of pseudomonas aeruginosa(PAO1) by this UVC phosphor at different irradiation times. The viability of *P. aeruginosa* PAO1 was only 39.6% after 16 min of X-ray irradiation, confirming its bactericidal ability.

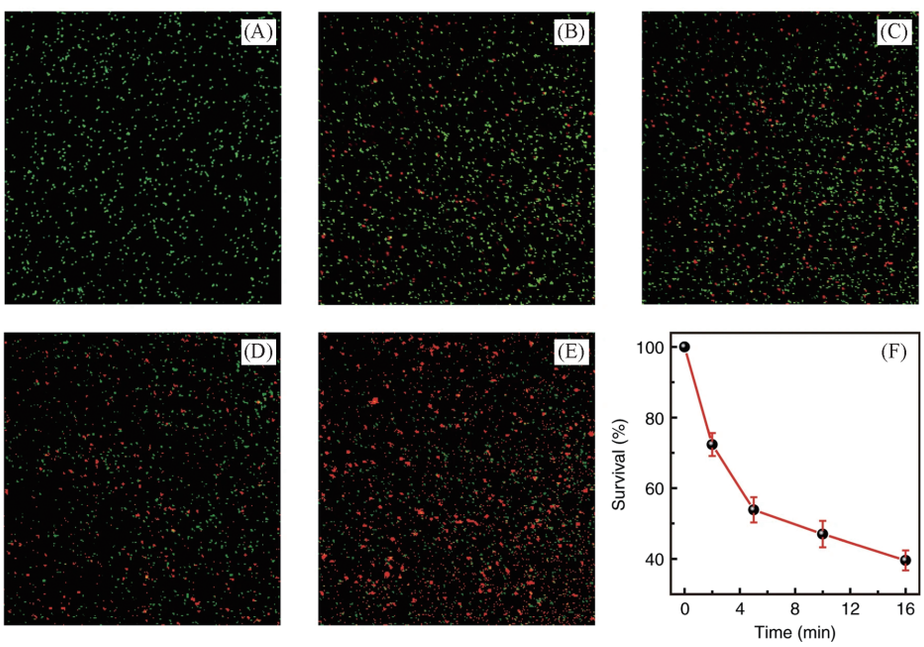

Fig. 3 Sterilization effect of UVC-LPP series on *P. aeruginosa* PAO1[77]

Confocal micrograph of the blank control group(A) and four LPPs inactivated PAO1 with different X-ray irradiation times of 2 min(B), 5 min(C), 10 min(D), and 16 min(E), where the green and red colors refer to the live and dead cells. (F) The relation curve between the time that LPPs exposure to X-ray irradiation and the corresponding survival ratios of PAO1, where 100% refers to the viability of PAO1 under natural conditions.

Copyright 2018, Springer Nature.

Li *et al.*[78] proposed a computational approach called topochemistry to replace the experimental attempt and guide the synthesis of UVC LPPs through in-depth studies of LPP defects(Fig. 4). By using first-principles density functional theory(DFT), they first calculated the formation energies of the various defects to discuss their possibility of becoming afterglow traps. They further evaluate the ability of traps to capture carriers by calculating the correspondent charge transfer levels for different defects under thermal activation. The results show that the introduction of composited vacancies and complicated defects contribute to the generation of superficial traps relating to valence and conduction bands. To test this hypothesis, they synthesized $La_{(1-x)}PO_4:xPr^{3+}$ with high-density oxygen and phosphorus vacancies by a solid-state reaction. After 600 s of exposure under X-ray irradiation, the phosphors indeed exhibited more than 2 h of UVC afterglow emission

with a maximum emission value of 231 nm. By using CaH_2 as an oxygenator to create more shadow traps in Pr^{3+} doped $LaPO_4$, they optimized the afterglow intensity of phosphors and proposed an afterglow mechanism based on defect concentration and free radical participation. Specifically, the ESR spectrum shows that there are a large number of $[PO_2]^{\cdot 2-}$ radicals in the monoclinic $LaPO_4$ crystals, which are obtained from the separation of two coordination oxygen atoms from $[PO_4]$ structure units. X-ray photons can interact with lattice atoms in the $[PO_2]^{\cdot 2-}$ radical, from where the high-energy electrons are ejected, accompanied by the formation of $[PO_2]^{\cdot 0}$ radicals, $O^{\cdot -}$ radicals and holes. And these generated charge carriers are then captured by oxygen divacancies in the lattice. Since the charge transfer level of oxygen is near the conduction band, the trapped electrons may escape from the traps and enter the conduction band at room temperature. Meanwhile, the holes can be coupled with Pr^{3+} ions. When the separated electrons drop to the 5*d* band of Pr^{3+} ions, the ions are excited to undergo transitions, resulting in the generation of UVC afterglows. This topological chemistry-based research method may provide theoretical guidance for the future discovery of new LPPs.

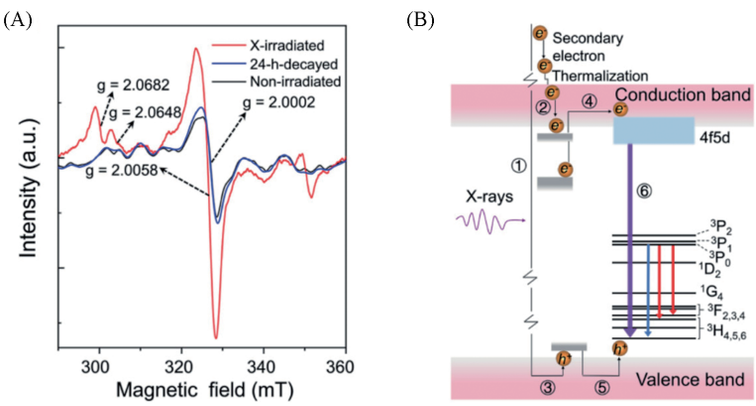

Fig. 4 Schematic sketch of the afterglow mechanism of Pr^{3+} doped $LaPO_4$ based on defect concentration and free radical participation[78]

(A) ESR spectra and 24 h decay of the Ca-144 h sample with and without X-ray irradiation, where 144 h means treated under 500 ℃ for 144 h. (B) Diagrammatic sketch of the radical implicated afterglow mechanism. The electron transitions are represented as black solid arrows. The electron and hole trap states are described as gray rectangles. The optical transitions of red, blue and UVC emissions are expressed as red, blue and purple arrows, respectively.

Copyright 2020, John Wiley and Sons.

5 Application of LPP Photocatalysis in Efficient Hydrogen Production

Hydrogen is a kind of promising clean energy with high calorific value and renewable characteristics, which is extensively utilized in the field of industrial production and transportation[79]. Hydrogen fuel cells can convert chemical energy from hydrogen and oxygen directly into electricity without any pollutant emissions, which is an ideal power supply for new energy vehicles[80]. However, hydrogen is inflammable and easy to explode. Besides, hydrogen atoms have a strong void effect, which makes it easy for them to infiltrate the metal crystal lattice, resulting in hydrogen embrittlement[81]. Hence, it is still a problem for hydrogen to store and transport safely. One efficient approach to work out this problem is to produce hydrogen on-site. However, hydrogen is mostly produced at high temperatures by hydrocarbon pyrolysis or water-gas shift (WGS) reactions, these processes require plenty of exterior heat. Field hydrogen production is still demanding. Photocatalysis can not only meet the requirement of field hydrogen generation, but also solve the related energy-economic problems. However, the highest solar-to-hydrogen (STH) conversion efficiency for particulate photocatalyst systems does not exceed 5% so far, which is still much less than the expected industrial standards of 10%[82,83]. Another limiting factor for the actual application of photocatalysis technology is that optoelectronic

materials or equipment without energy storage devices are not able to work under dark conditions. Fortunately, LPPs offer a new way to overcome these restrictions.

Cui *et al.* [84] directly applied the long persistent material to photocatalytic hydrogen production and achieve a 5.18% theoretical STH conversion (Fig. 5). They synthesized a micrometer-sized brick-shaped $Sr_2MgSi_2O_7$: Eu^{2+}, Dy^{3+} material by the sol-gel method. The doped Eu^{2+} and Dy^{3+} ions occupy the Sr^{2+} center of the $Sr_2MgSi_2O_7$, causing lattice distortion of the $Sr_2MgSi_2O_7$ matrix and producing a large number of surface defects. The existence of these lattice defects is generally considered to be beneficial to improve photocatalytic activity. The synthesized long persistent material exhibited long afterglow emission under UV excitation, with the strongest signal peak at 465 nm. After 15 min of UV irradiation, the hydrogen production accumulated continuously within 8 h and reached 264 μmol/g, with an STH conversion efficiency of 0.39%. Unique carrier migration pathways also contribute to its excellent photocatalytic hydrogen evolution performance. To be more specific, the excited carrier migration pathway is shown in Fig. 6. The electrons of Eu^{2+} are firstly excited from the ground-state 4*f* to the 5*d* level, where they are further excited by thermal energy and migrate to the conduction band (CB) of the host material $Sr_2MgSi_2O_7$. Hence, Eu^{2+} changes into Eu^{3+} and the excited electrons in CB will be captured by Dy^{3+}, accompanied by the formation of Dy^{2+}. In the process of photocatalytic reaction under illumination, the majority of excited Eu^{2+} electrons in CB can directly react with the substrates, while the unconsumed ones can keep on transferring. These transferred electrons will then be captured and stored by Dy^{3+} ions temporarily, resulting in a longer carrier lifetime and improved catalytic efficiency in light conditions.

Liu *et al.* [85] used g-C_3N_4@Au@$SrAl_2O_4$: Eu^{2+}, Dy^{3+} composites as an efficient plasmonic photocatalyst to realize environmental purification and hydrogen production simultaneously (Fig. 6). They firstly embedded Au nanoparticles into g-C_3N_4 by Pechini-type sol-gel process, and then mechanically coated g-C_3N_4@Au composites on the surface of $SrAl_2O_4$: Eu^{2+}, Dy^{3+} long persistent phosphors under high-temperature calcination

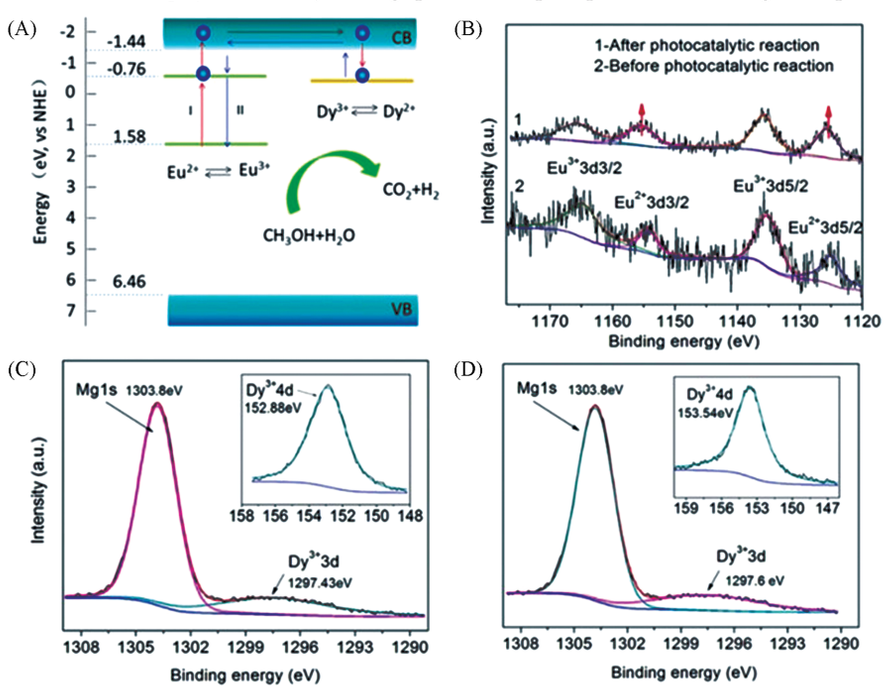

Fig. 5 Diagrammatic sketch of the mechanism of $Sr_2MgSi_2O_7$: Eu^{2+}, Dy^{3+} participated in the photocatalysis process[84]

(A) Simple description of energy levels and photoinduced electron transfer processes. (B)—(D) XPS spectra of Eu_{3d}, Dy_{3d} and Dy_{4d} to demonstrate their behavior throughout the photocatalysis process.

Copyright 2019, John Wiley and Sons.

conditions to obtain the g-C_3N_4@Au@$SrAl_2O_4$: Eu^{2+}, Dy^{3+} composites. Because nanoparticles of noble metals such as Au have strong photo-material interaction properties[86]. Local surface plasmon resonance(LSPR) phenomenon occurs when g-C_3N_4@Au plasmonic photocatalyst composites interact with photons that match the surface valence electron collective oscillation frequency. At this point, strong electromagnetic fields and high energy carriers of a high concentration will be generated on the surface of g-C_3N_4@Au nanostructures. Owing to the continuous and effective supply of high-energy carriers under LSPR excitation, direct transfer of positive and negative charges occurs between the plasma noble metal nanoparticles and the original photocatalyst at the interface, thus the g-C_3N_4 pristine photocatalysts will have significant photocatalytic activity for hydrogen production. Moreover, the additional local electromagnetic field formed in the composites promotes the formation, migration, and separation of photogenerated carriers, thus obviously improves the photocatalytic efficiency of the composite. This process is called the near-field electromagnetic effect. In combination with $SrAl_2O_4$: Eu^{2+}, Dy^{3+} long persistent phosphors, the g-C_3N_4@Au@$SrAl_2O_4$: Eu^{2+}, Dy^{3+} composite can maintain the catalytic activity for about 3 h after the excitation light source(visible light) is turned off and continues to produce about 3 μmol of hydrogen.

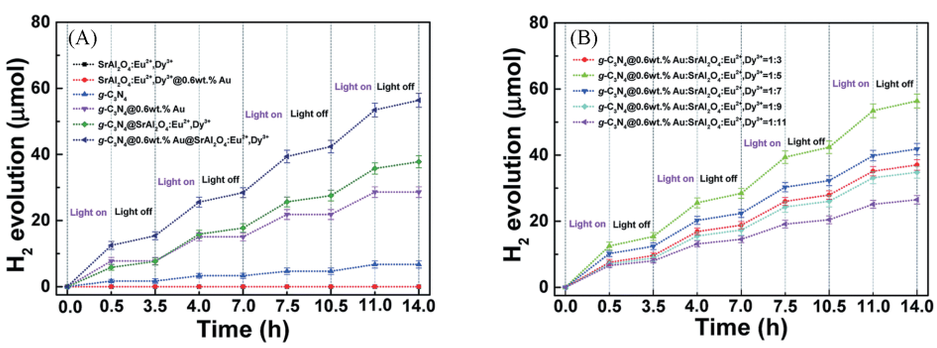

Fig. 6 Comparison of hydrogen generation process of the pristine g-C_3N_4, $SrAl_2O_4$: Eu^{2+}, Dy^{3+} LPP, $SrAl_2O_4$:Eu^{2+}, Dy^{3+}@Au, g-C_3N_4@Au, g-C_3N_4@$SrAl_2O_4$:Eu^{2+}, Dy^{3+}, and g-C_3N_4@Au@$SrAl_2O_4$:Eu^{2+}, Dy^{3+} composites(A), comparison of hydrogen generation process of g-C_3N_4@Au@x$SrAl_2O_4$:Eu^{2+}, Dy^{3+} composites with different mass fractions(B)[85]

Copyright 2019, Royal Society of Chemistry.

6 Conclusions and Prospects

Persistent phosphor is a new luminescent material with electron storage capacity, which has attracted wide attention in the field of photocatalysis. In this review, we discuss the application of long afterglow phosphors in organic degradation, sterilization, and catalytic hydrogen production. Persistent phosphors have special advantages in round-the-clock photocatalysis because it does not require the aid of an external light source. And due to its long decay time, it can maintain a long photocatalytic activity once it is charged. In the past few years, different kinds of long persistent phosphors have been rationally designed to improve the sustained luminescence intensity and increase the decay time for better photocatalytic performance.

Although great progress has been made, the application of long persistent phosphors in sterilization and hydrogen production is still in its infancy. At the present stage, long persistent phosphors for hydrogen production still face the problems of low optical conversion rate and short carrier life, so it is very important to develop composites with wide spectral utilization range and deep trap level. Meanwhile, the high-efficiency photocatalytic strategy and method based on long persistent phosphors need to be developed, and more progress of long persistent phosphors in hydrogen production is still worth looking forward to. Also, for UV long persistent phosphors applied in sterilization and disinfection, there are still several problems to be solved: (1)

because UV light is not visible, there is an urgent need for a more standardized method to measure and define the performance of UV persistent phosphors, such as the luminescence duration, so that the experimental results of the same or different phosphor compositions by different research groups are comparable. (2) An empirical energy level map based on the link between trap concentration and depth and luminescence band is needed to predict new long persistent phosphors and select suitable co-doping agents accordingly. In summary, the long persistent phosphors exhibit unprecedented advantages in photocatalysis, providing new possibilities for future applications in the field of environment and energy.

This paper is supported by the Natural Science Foundation of Hunan Province, China(Nos.2020JJ4173, 2020JJ5038), the Technology Innovation Program of Hunan Province, China (No. 2018RS3060) and the Changsha Municipal Science and Technology Projects, China(No. kq1901030).

References

[1] Li Y., Gecevicius M., Qiu J., *Chem. Soc. Rev.*, **2016**, *45*(8), 2090—2136
[2] Matsuzawa T., Aoki Y., Takeuchi N., Murayama Y., *J. Electrochem. Soc.*, **1996**, *143*(8), 2670—2673
[3] van den Eeckhout K., Smet P. F., Poelman D., *Materials*, **2010**, *3*(4), 2536—2566
[4] Zirkle C., *Isis*, **1959**, *50*(1), 68, 69
[5] Sidot. M., *C R Acad. Sci. Paris*, **1866**, *62*, 999—1001
[6] Smet P. F., Moreels I., Hens Z., Poelman D., *Materials*, **2010**, *3*(4), 2834—2883
[7] Wang Y., Gong Y., Xu X., Li Y., *J. Lumin.*, **2013**, *133*, 25—29
[8] Smet P. F., Botterman J., van den Eeckhout K., Korthout K., Poelman D., *Opt. Mater.*, **2014**, *36*(11), 1913—1919
[9] Smet P. F., Viana B., Tanabe S., Peng M., Hölsä J., Chen W., *Opt. Mater. Express*, **2016**, *6*(4), 1414—1419
[10] Lin Z., Kabe R., Nishimura N., Jinnai K., Adachi C., *Adv. Mater.*, **2018**, *30*(45), 1803713
[11] Lin Q., Li Z., Yuan Q., *Chin. Chem. Lett.*, **2019**, *30*(9), 1547—1556
[12] Liu Y., Wang Y., Jiang K., Sun S., Qian S., Wu Q., Lin H., *Talanta*, **2020**, *206*, 10.1016/j.talanta.2019.120206
[13] Zhang Y., Huang R., Li H., Lin Z., Hou D., Guo Y., Song J., Song C., Lin Z., Zhang W., Wang J., Chu P. K., Zhu C., *Small*, **2020**, e2003121
[14] Zeng W., Wang Y., Zheng M., Yang R., Luo Y., Yi X., Zhang R., *J. Alloys Compd.*, **2020**, *825*, 10.1016/j.jallcom.2020.154143
[15] Zhang H., Zhao L., Tian S., Yang X., Liu Z., Yu X., Yang X., Zhang M., Qiu J., Xu X., *J. Non-Cryst. Solids*, **2020**, *533*, 10.1016/j.jnoncrysol.2019.119830
[16] Wu S., Li Y., Ding W., Xu L., Ma Y., Zhang L., *Nano-Micro Lett.*, **2020**, *12*(1), 10.1007/s40820-020-0404-8
[17] Schneider J., Matsuoka M., Takeuchi M., Zhang J. L., Horiuchi Y., Anpo M., Bahnemann D. W., *Chem. Rev.*, **2014**, *114*(19), 9919—9986
[18] Linsebigler A. L., Lu G., Yates J., J T, *Chem. Rev.*, **1995**, *95*(3), 735—758
[19] Cai T., Liu Y., Wang L., Dong W., Zeng G., *J. Photochem. Photobiol. C*, **2019**, *39*, 58—75
[20] Zhang J. Y., Pan F., Hao W., Ge Q., Wang T. M., *Appl. Phys. Lett.*, **2004**, *85*(23), 5778—5780
[21] Fang Y., Ma Y., Zheng M., Yang P., Asiri A. M., Wang X., *Coord. Chem. Rev.*, **2018**, *373*, 83—115
[22] Jin X., Ye L., Xie H., Chen G., *Coord. Chem. Rev.*, **2017**, *349*, 84—101
[23] Knoer G., *Coord. Chem. Rev.*, **2015**, *304*, 102—108
[24] Maeda K., *ACS Catal.*, **2013**, *3*(7), 1486—1503
[25] Fox M. A., Dulay M. T., *Chem. Rev.*, **1993**, *93*, 1, 341—357
[26] Cheng B., Zhang Z., Han Z., Xiao Y., Lei S., *Crystengcomm*, **2011**, *13*(10), 3545—3550
[27] Dong G., Xiao X., Zhang L., Ma Z., Bao X., Peng M., Zhang Q., Qiu J., *J. Mater. Chem.*, **2011**, *21*(7), 2194—2203
[28] Hou C., Wang Y., Zhu H., Zhou L., *J. Mater. Chem. B*, **2015**, *3*(14), 2883—2891
[29] Le Masne de Chermont Q., Chanac C., Seguin J., Pelle F., Maitrejean S., Jolivet J. P., *Liver Transplant.*, **2007**, *13*(11), 1604—1604
[30] Luo H., Bos A. J. J., Dobrowolska A., Dorenbos P., *Phys. Chem. Chem. Phys.*, **2015**, *17*(23), 15419—15427
[31] Smet P. F., Avci N., Van den Eeckhout K., Poelman D., *Opt. Mater. Express*, **2012**, *2*(10), 1306—1313
[32] Teng Y., Zhou J., Khisro S. N., Zhou S., Qiu J., *Mater. Chem. Phys.*, **2014**, *147*(3), 772—776
[33] Xia Z., Li Q., Li G., Xiong M., Liao L., *J. Cryst. Growth*, **2011**, *318*(1), 958—961
[34] Yoshimura F., Nakamura K., Wakai F., Hara M., Yoshimoto M., Odawara O., Wada H., *Appl. Surf. Sci.*, **2011**, *257*(6), 2170—2175
[35] Wang Y. H., Wang L., Zhang S. H., *Chem. J. Chinese Universities*, **2005**, *26*(11), 1990—1993
[36] Liu H., Hu X., Wang J., Liu M., Wei W., Yuan Q., *Chin. Chem. Lett.*, **2018**, *29*(11), 1641—1644
[37] Brito H. F., Holsa J., Laamanen T., Lastusaari M., Malkamaki M., Rodrigues L. C. V., *Opt. Mater. Express*, **2012**, *2*(4), 371—381
[38] Wang J., Ma Q., Wang Y., Shen H., Yuan Q., *Nanoscale*, **2017**, *9*(19), 6204—6218

[39] Li Y., Zhou S., Dong G., Peng M., Wondraczek L., Qiu J., *Sci. Rep.*, **2014**, *4*, 4059
[40] Sakar M., Nguyen C., Vu M., Do T., *ChemSusChem*, **2018**, *11*(5), 809—820
[41] Li F., Li Z., Cai Y., Zhang M., Shen Y., Wang W., *Mater. Lett.*, **2017**, *208*, 111—114
[42] Li H., Yin S., Wang Y., Sato T., *Environ. Sci. Technol.*, **2012**, *46*(14), 7741—7745
[43] Li H., Yin S., Wang Y., Sato T., *J. Catal.*, **2012**, *286*, 273—278
[44] Li H., Yin S., Wang Y., Sato T., *RSC Adv.*, **2012**, *2*(8), 3234—3236
[45] Li H., Yin S., Wang Y., Sato T., *Appl. Catal. B*, **2013**, *132*, 487—492
[46] Zhou Q., Peng F., Ni Y., Kou J., Lu C., Xu Z., *J. Photochem. Photobiol. A*, **2016**, *328*, 182—188
[47] Sui D., Chai Y., *Chem. Lett.*, **2017**, *46*(4), 516—519
[48] Fan H. T., Zhao C. Y., Liu S., Shen H., *J. Chem. Eng. Data*, **2017**, *62*(3), 1099—1105
[49] Vandezande P., Gevers L. E. M., Vankelecom I. F. J., *Chem. Soc. Rev.*, **2008**, *37*(2), 365—405
[50] Solis M., Solis A., Ines Perez H., Manjarrez N., Flores M., *Process Biochem.*, **2012**, *47*(12), 1723—1748
[51] Panizza M., Cerisola G., *Water Res.*, **2009**, *43*(2), 339—344
[52] Wang C., Li J., Lv X., Zhang Y., Guo G., *Energy Environ. Sci.*, **2014**, *7*(9), 2831—2867
[53] Li X., Yu J., Jaroniec M., *Chem. Soc. Rev.*, **2016**, *45*(9), 2603—2636
[54] Li H., Yin S., Sato T., *Appl. Catal. B*, **2011**, *106*(3/4), 586—591
[55] Yin H., Chen X., Hou R., Zhu H., Li S., Huo Y., Li H., *ACS Appl. Mater. Interfaces*, **2015**, *7*(36), 20076—20082
[56] Huo Y., Chen X., Zhang J., Pan G., Jia J., Li H., *Appl. Catal. B*, **2014**, *148*, 550—556
[57] Huo Y., Hou R., Chen X., Yin H., Gao Y., Li H., *J. Mater. Chem. A*, **2015**, *3*(28), 14801—14808
[58] Li K., Zhang H., He Y., Tang T., Ying D., Wang Y., Sun T., Jia J., *Chem. Eng. J.*, **2015**, *268*, 10—20
[59] Liu M., Sunada K., Hashimoto K., Miyauchi M., *J. Mater. Chem. A*, **2015**, *3*(33), 17312—17319
[60] Yu Z., Li F., Sun L., *Energy Environ. Sci.*, **2015**, *8*(3), 760—775
[61] Zhou J., Huang J., Xia Y., Ou H., Li Z., *Sci. Total Environ.*, **2020**, *699*, 10.1016/j.scitotenv.2019.134342
[62] Wu H., Wang Z., Koike K., Negishi N., Jin Y., *Catal. Sci. Technol.*, **2017**, *7*(17), 3736—3746
[63] Lu Y., Zhang X., Chu Y., Yu H., Huo M., Qu J., Crittenden J. C., Huo H., Yuan X., *Appl. Catal. B*, **2018**, *224*, 239—248
[64] Elimelech M., Phillip W. A., *Science*, **2011**, *333*(6043), 712—717
[65] Flemming H., Schaule D., Griebe T., Schmitt J., Tamachkiarowa A., *Desalination*, **1997**, *113*(2—3), 215—225
[66] Kang G., Gao C., Chen W., Jie X., Cao Y., Yuan Q., *J. Membr. Sci.*, **2007**, *300*(1/2), 165—171
[67] Johnson T. A., Rehak E. A., Sahu S. P., Ladner D. A., Cates E. L., *Environ. Sci. Technol.*, **2016**, *50*(21), 11912—11921
[68] Kadyan S., Singh S., Simantilleke A. P., Singh D., *Optik*, **2020**, *212*, 10.1016/j.ijleo.2020.164671
[69] AbdukaderA., Renagul A., Ailijiang T., Adil M., *Chem.J. Chinese Universities*, **2016**, *37*(5), 810—816
[70] De Guzman GNA., Fang M., Liang C., Bao Z., Hu S., Liu R., *J. Lumin.*, **2020**, *219*, 10.1016/j.jlumin.2019.116944
[71] Wang B., Chen Z., Li X., Zhou J., Zeng Q., *J. Alloys Compd.*, **2020**, *812*, 10.1016/j.jallcom.2019.152119
[72] Puxian X., Mingying P., *Opt. Mater. X*, **2019**, *2*, 100022
[73] Li Z., Li H., Sun H., *J. Rare Earths*, **2020**, *38*(2), 124—129
[74] Sun H., Gao Q., Wang A., Liu Y., Wang X., Liu F., *Opt. Mater. Express*, **2020**, *10*(5), 1296—1302
[75] Yan S., Liu F., Zhang J., Wang X., Liu Y., *Phys. Rev. Appl.*, **2020**, *13*(4), 10.1103/PhysRevApplied.13.044051
[76] Wang X., Chen Y., Liu F., Pan Z., *Nat. Commun.*, **2020**, *11*(1), 10.1038/s41467-020-16015-z
[77] Yang Y., Li Z., Zhang J., Lu Y., Guo S., Zhao Q., Wang X., Yong Z., Li H., Ma J., Kuroiwa Y., Moriyoshi C., Hu L., Zhang L., Zheng L., Sun H., *Light: Sci. Appl.*, **2018**, *7*, 88
[78] Li H., Liu Q., Ma J., Feng Z., Liu J., Zhao Q., Kuroiwa Y., Moriyoshi C., Ye B., Zhang J., Duan C., Sun H., *Adv. Opt. Mater.*, **2020**, *8*(4), 1901727
[79] Tee S. Y., Win K. Y., Teo W. S., Koh L., Liu S., Teng C. P., Han M., *Adv. Sci.*, **2017**, *4*(5), 1600337
[80] Jacobson M. Z., Colella W. G., Golden D. M., *Science*, **2005**, *308*(5730), 1901—1905
[81] Dutta S., *J. Ind. Eng. Chem.*, **2014**, *20*(4), 1148—1156
[82] Li R., *Chin. J. Catal.*, **2017**, *38*(1), 5—12
[83] Wang Q., Hisatomi T., Jia Q., Tokudome H., Zhong M., Wang C., Pan Z., Takata T., Nakabayashi M., Shibata N., Li Y., Sharp I., Kudo A., Yamada T., Domen K., *Nat. Mater.*, **2016**, *15*(6), 611—615
[84] Cui G., Yang X., Zhang Y., Fan Y., Chen P., Cui H., Liu Y., Shi X., Shang Q., Tang B., *Angew. Chem., Int. Ed.*, **2019**, *58*(5), 1340—1344
[85] Liu X., Chen X., Li Y., Wu B., Luo X., Ouyang S., Luo S., Al Kheraif A. A., Lin J., *J. Mater. Chem. A*, **2019**, *7*(32), 19173—19186
[86] Wang C., Nie X., Shi Y., Zhou Y., Xu J., Xia X., Chen H., *ACS Nano*, **2017**, *11*(6), 5897—5905

(Ed.: V, K)